Fatigue & Fracture of
Engineering Materials & Structures

doi:10.1111/j.1460-2695.2008.01259.x

Use of the small punch test to determine the ductile-to-brittle transition temperature of structural steels

M. A. CONTRERAS, C. RODRÍGUEZ, F. J. BELZUNCE and C. BETEGÓN

Escuela Politécnica Superior de Ingeniería de Gijón, Universidad de Oviedo, Campus de Viesques, 33203 Gijón, España

Received in final form 23 June 2008

ABSTRACT The small punch test (SPT) consists in punching very small square specimens, measuring 10×10 mm^2 and 0.5-mm thickness, until fracture using a 2.5-mm-diameter hemispherical punch. Different specimens of a structural steel were tested from room temperature to cryogenic temperatures in order to determine its ductile-to-brittle transition temperature (DBTT). The DBTT obtained in SPT ($DBTT_{STP}$) is much lower than the DBTT obtained by means of Charpy specimens ($DBTT_{CVN}$). The variation of the mechanical parameters calculated from the SPTs with temperature was also calculated and the operative fracture micromechanisms defined using a scanning electron microscope.

Keywords ductile-to-brittle transition temperature (DBTT); miniature tests; small punch test (SPT); structural steels.

NOMENCLATURE

A = tension test elongation
CVN = Charpy V-notch test
d = load point displacement or specimen deflexion
DBTT = ductile-to-brittle transition temperature
$DBTT_{CVN}$ = ductile-to-brittle transition temperature obtained by means of Charpy-V tests
$DBTT_{CVN50\%}$ = ductile-to-brittle transition temperature corresponding to the mean value of the upper shelf energy in Charpy-V tests
$DBTT_{CVN28J}$ = ductile-to-brittle transition temperature corresponding to an energy value of 28J in Charpy-V tests
$DBTT_{CVN41J}$ = ductile-to-brittle transition temperature corresponding to an energy value of 41J in Charpy-V tests
$DBTT_{FATT}$ = ductile-to-brittle transition temperature corresponding to a 50% brittle fracture appearance
$DBTT_{SPT}$ = ductile-to-brittle transition temperature corresponding to the mean value of the upper shelf energy in SPT tests
d_f = load point displacement at fracture
d_{max} = load point displacement at maximum load
P_{max} = maximum load
P_y = load needed to initiate general plastic deformation
SPT = small punch test
t = specimen initial thickness

Correspondence: C. Rodríguez. E-mail: cristina@uniovi.es

This manuscript is based on a presentation made at the XXIV Spanish Fracture Group meeting held in Burgos 2007.

T = Temperature
t_f = specimen thickness at fracture
W_f = energy at fracture
W_{max} = energy at maximum load
Z = % area reduction in the tension test
$\alpha, \alpha_1, \alpha_2$ = characteristic constants
β_1, β_2 = characteristic constants
ε_f = strain at the failure region
γ = characteristic constant
σ_{ys} = yield stress
σ_u = tensile strength

INTRODUCTION

The mechanical properties evaluation of structural components of thermal and nuclear power stations and their degradation during their service life due to temperature, neutron irradiation, etc., are fundamental aspects to take into account when assessing the structural integrity of these units and their expected residual lives.[1]

Standard mechanical characterization is always destructive, as relatively large specimens need to be machined from the real component for the evaluation. In the aforementioned situations, it would be very convenient to use miniature tests for the mechanical characterization of materials, making use of very small specimens which could be extracted from the components during their normal service life. One of these tests is the small punch test (SPT). As the SPT uses small square specimens measuring $10 \times 10\ mm^2$ with a thickness of 0.5 mm, it may be considered a quasi non-destructive test.[2] In this test, the square specimen is firmly clamped between two circular dies and is strained until failure into a 4-mm-diameter cavity using a 2.5-mm-diameter hemispherical punch, as shown in Fig. 1. The load applied is graphically plotted against the deflection of the specimen central point (Fig. 2). The figure shows a typical curve, on which are marked different zones corresponding to the different states of deformation that the specimen will suffer.

Zones I and II correspond to states of bending deformation. Zone I corresponds to elastic bending and includes the linear portion of the curve, while zone II corresponds to plastic bending. For specimens of standardized geometry and for the same testing machine, these curves are determined by the elastic–plastic material properties, i.e. the elastic modulus, yield stress σ_{ys} and hardening coefficient of the material. From a certain moment onward, bending leads to a membrane regime, which predominates in most of the curve and corresponds to zone III. This phase ends with fracture of the specimen. In the curve represented in Fig. 2, final fracture occurs as a result of the formation of a neck similar to that developed in tension tests of ductile materials and the subsequent formation of a crack in this location. At lower temperatures, zone III is smaller, because the fracture is produced at smaller displacement and may even occur in zone II of the curve, without

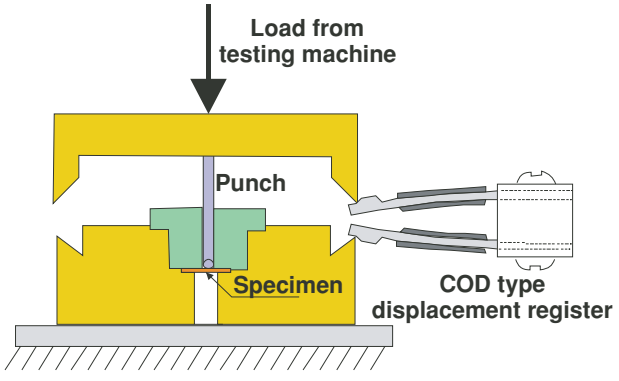

Fig. 1 Schematic representation of the SPT equipment.

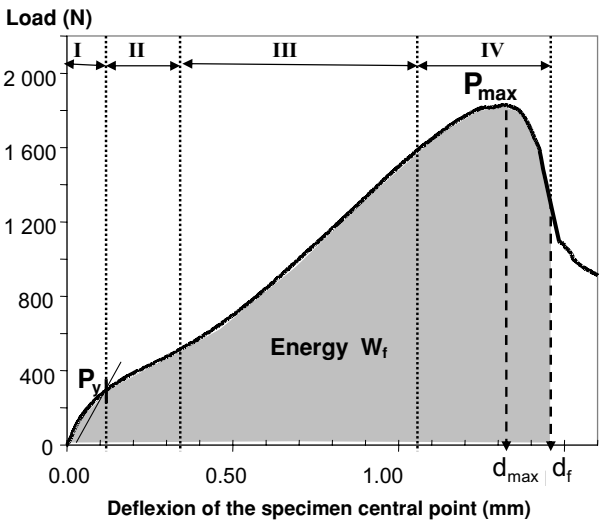

Fig. 2 SPT load-deflection curve and identification of critical parameters.

membrane deformation actually starting. In any case, fracture of the specimen defines zone IV, which includes the point of maximum load. In addition to the mechanical properties of the material, this point of maximum load depends on the coefficient of friction between the punch and the sample being tested, such that the higher this coefficient is, the greater the load and fracture location moved away from the centre of the dome.[3]

This load-displacement curve is the only information collected in the SPT and thus the only one at our disposal to ascertain the different material properties. Due to the complexity of the stress state that develops during the test, the work developed so far has focused on establishing empirical relationships between different mechanical properties and certain characteristic points of the curves,[2,4] also marked on the curve in Fig. 2. For example, the first two parts of the curve are used to obtain the parameters of the plastic stress–strain curve of the material. In particular, the value of the yield stress is related to the load P_y, through relationships of the type

$$\sigma_{ys} = \alpha_1 + \alpha_2\left(\frac{P_y}{t^2}\right), \tag{1}$$

α_1 and α_2 being constants which depend on the type of material, t the thickness of the specimen and P_y the load at the beginning of the plastic bending regime.

Fracture properties are related to zone IV of the curve. In particular, the tensile strength, σ_u, is related to the maximum load in the test, P_{max}, through expressions such as

$$\sigma_u = \beta_1 + \beta_2\left(\frac{P_{max}}{t^2}\right), \tag{2}$$

where β_1 and β_2 are constants which depend on the type of material and the coefficient of friction. The displacements at maximum load, d_{max}, and at fracture, d_f, are related to the tensile elongation of the material. The enclosed area below the curve up to these two displacements defines the maximum load energy and the fracture energy, W_{max} and W_f, respectively. Fracture strain may also be defined from experimental measurement of the final thickness of the specimen in the necking region as follows:

$$\epsilon_f = \ln(t/t_f), \tag{3}$$

where t_f is the thickness at the fracture location of the specimen.

Another important property of structural steels is the so-called ductile-to-brittle transition temperature associated with the temperature at which the fracture behaviour of the material changes from ductile to brittle. Different researchers have already used the SPT to define the ductile-to-brittle transition temperature (DBTT) of ferritic steels.[5,6] SPTs may be performed from room to cryogenic temperatures, plotting the absorbed energy until rupture W_f, against the test temperature. As in the case of Charpy tests (CVN), a ductile region (high energy) and a brittle region (low energy) with a gentle transition between both zones are usually reported.[7]

The transition temperature thus obtained, $DBTT_{SPT}$, is also related through empirical expressions to the transition temperature obtained in CVN tests, $DBTT_{CVN}$, or in fracture toughness testing. Different researchers[5,6,8] have used linear expressions such as

$$DBTT_{SPT} = \gamma\ DBTT_{CVN}, \tag{4}$$

where γ is a material characteristic constant. In all cases, the $DBTT_{SPT}$ temperature is much lower than that obtained in the CVN tests.

In this work, we have carried out SPTs at different temperatures on a ferritic-perlitic high toughness steel: the structural steel AE460. On the one hand, the SPT transition temperature for this steel is obtained, and associated with the same temperature obtained in a CVN test. Moreover, we studied the ability of SP test to get the conventional mechanical properties of this material at different temperatures, establishing relationships between these properties and characteristic points of the load-displacement test at different temperatures. For this reason, an experimental programme was conducted on the structural steel, in which, in addition to the SP tests, CVN tests and tensile tests at different temperature have been performed.

MATERIALS AND EXPERIMENTAL PROCEDURES

A microalloyed ferritic-pearlitic structural steel AE460 was used in this study. The steel was supplied in the as-hot rolled condition. Its chemical composition is shown in Table 1.

Tensile tests were performed on cylindrical specimens with a diameter of 6 mm and 50 mm of gauge length. The tests were carried out using an INSTRON 5582 servo-hydraulic machine at constant nominal strain rates of 2×10^{-4} s^{-1} in the temperature range from -60 °C to $+50$ °C. The low temperature tests were performed by means of an ambient chamber cooled with liquid nitrogen.

Table 1 Chemical composition of the AE460 steel

%C	%Si	%Mn	%P	%S	%Al	%Ni	%Nb	%V
0.18	0.41	1.54	0.015	0.002	0.071	0.47	0.057	0.14

CVN impact tests were performed using standard 2 mmV-notch Charpy specimens ($55 \times 10 \times 10$ mm^3) in an Ibertest impact machine. Low temperature tests were performed either using an ambient chamber cooled with liquid nitrogen. Also a resistance heated chamber was used in order to cover a temperature range from −196 to +80 °C.

SPT specimens of 1-mm thickness were machined from longitudinal Charpy specimens using a precision metallurgical cut-off machine. These specimens were mechanically ground and finally polished using 6-μm grit diamond paste in order to obtain the same thickness ($t = 0.5$ mm) and the same surface finish in all the samples under test. This will eliminate the dependence of the results on two test variables, such as thickness and the coefficient of friction. In order to further decrease the effects of the latter variable, the tests were conducted lubricating the contact zone between the punch and the specimen.

SPTs were performed using a special device designed and manufactured in our own laboratory, which was attached to a static mechanical machine with a load cell capacity of 10 kN. Figure 1 shows the testing equipment, which is better described in Autillo *et al.*[9] As the displacement measured by means of the extensometer also includes the deformation of all the equipment tools, additional tests were performed on a rigid material so as to ascertain the compliance of our testing device, correct the experimental curves, and thus obtain the real load-displacement curves of the tested specimens.

SPTs were carried out from −140 °C to ambient temperature. Low temperature tests were performed by placing the experimental device described above in an ambient chamber cooled with liquid nitrogen. A thermocouple situated at a distance of less than 2 mm from the lower face of the specimen was used to obtain an accurate measure of the specimen temperature during the test.

All the tests were conducted under a punch displacement rate of 0.2 mm/min and were ended when the applied load attained a value 50% lower than the maximum registered load, so as to have a visible crack on the test specimen. At the end of the tests, all the fracture surfaces of the specimens were observed under a scanning electron microscope. Finally, they were resin mounted, diametrically cut and the thickness of the failure region was measured under a stereoscopic magnifier.

RESULTS

Figure 3 shows some of the SPT curves obtained at different temperatures. Two aspects are worth highlighting: first, the lower the temperature, the greater the load needed to attain a certain deformation; and second, at the lowest temperatures, there is a substantial decrease in failure displacement and specimen failure takes place suddenly.

As already mentioned, the area below the load-displacement curve until failure corresponds to the energy absorbed in the test. In the case of brittle behaviour (e.g. −130 and −140 °C in Fig. 3), failure was defined when the first sudden drop in the load took place. Energy at failure was represented in Fig. 4 against test temperature and clearly shows the typical ductile-to-brittle transition, similar to that existing in CVN tests. The SPT high energy region of this steel extends for $T \geq -100$ °C and

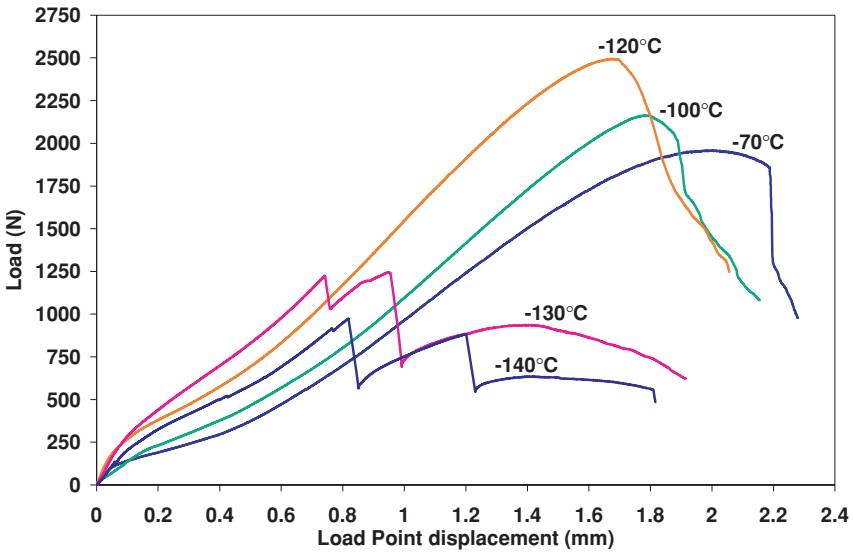

Fig. 3 AE460 SPT curves at different test temperatures.

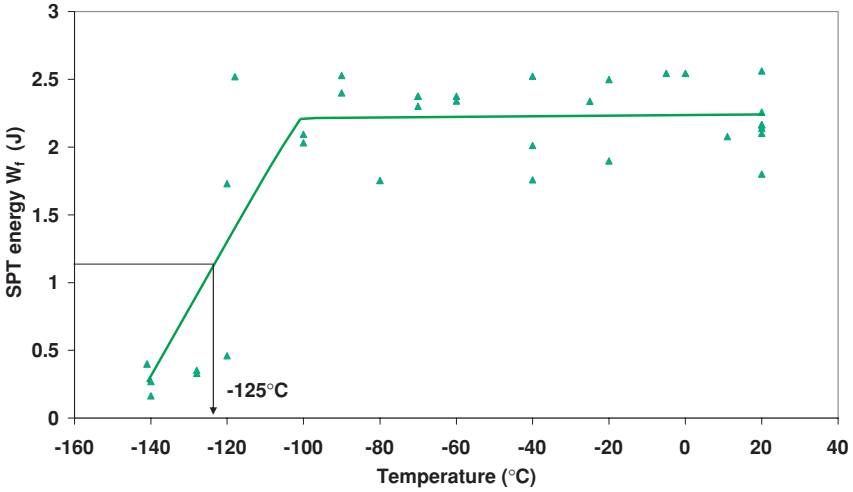

Fig. 4 SPT transition curve (AE460 steel).

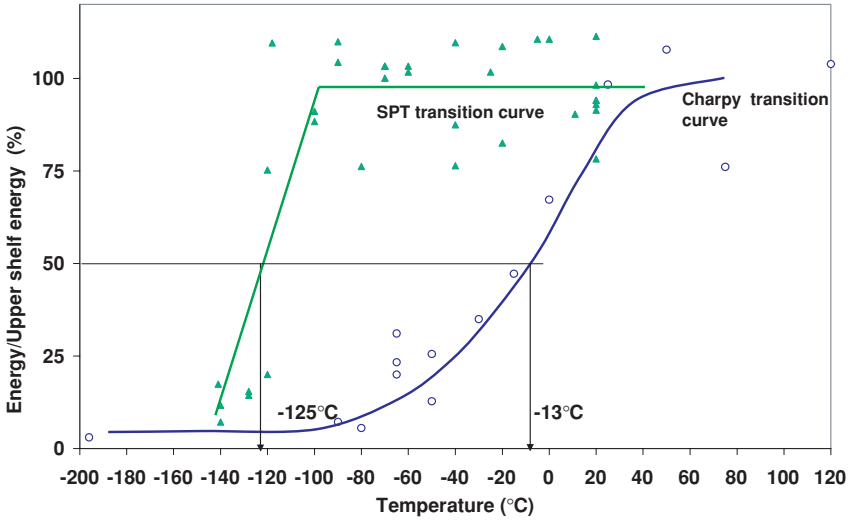

Fig. 5 SPT and Charpy transition curves (AE460 steel).

the SPT low energy region starts at temperatures below −140 °C.

Figure 5 shows the ductile-to-brittle transition curves obtained using both small punch and standard CVN tests. In order to compare the curves, they were adimensionalized by dividing the obtained energy in each test by the mean fracture energy corresponding to the upper shelf of each type of test.

As can be seen, SPT ductile-to-brittle transition occurs in a lower range of temperatures than in the CVN test. By means of this representation, it is possible to use a similar criterion to define the transition temperature in both tests. Assuming one of the criteria usually used in the case of the Charpy transition curves, we calculated the transition temperature as the temperature corresponding to an energy value equal to half of the ductile region energy (temperature corresponding to the 50% energy value in Fig. 5). A transition temperature of −125 °C was obtained for the SPTs and a value of −13 °C for the CVN tests.

As can be seen in Fig. 6, the ductile-to-brittle transition can also be clearly observed by representing the strain measured on the failure region versus temperature, although the dispersion is much higher in this case. It should be noted that the range of temperatures corresponding to the brittle-to-ductile transition is greater than in the case of energy. As shown in Fig. 6, transition begins at a higher temperature (about −90 °C) than when the energy plot was used, and the brittle region now starts at −130 °C. Figure 7 shows two specimens, tested at different temperatures, and cut diametrically so as to show the deformation measurement on the failure region.

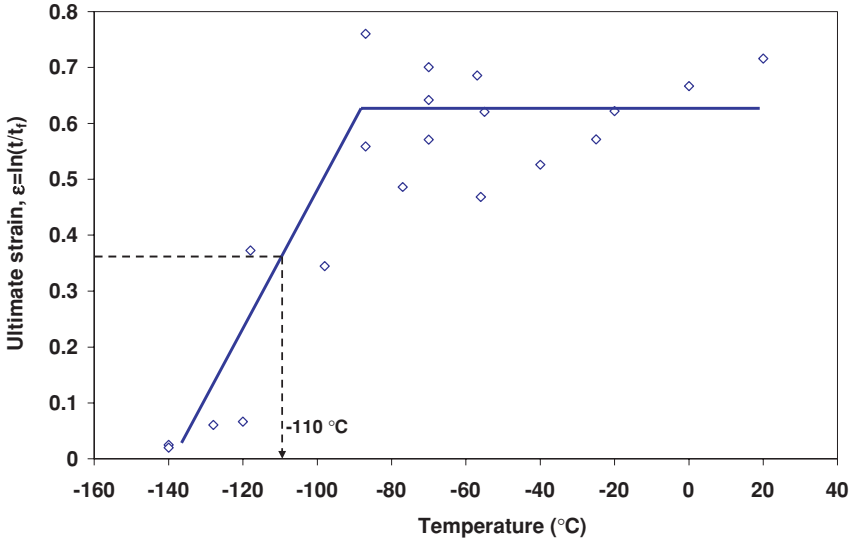

Fig. 6 SPT fracture strain representation versus temperature (AE460).

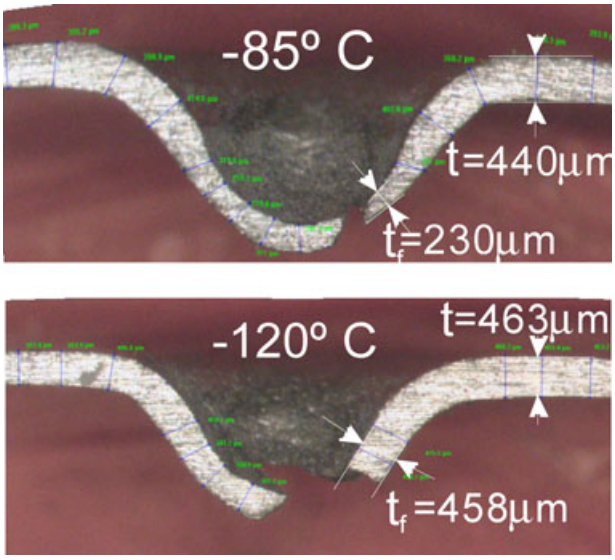

Fig. 7 Low temperature SPT failed specimens.

The first temperature, −85 °C, corresponds to the ductile plateau of the transition curve. The figure shows the point where the thickness at failure was measured. As can be seen, it is clearly smaller than the failure thickness at a temperature of −120 °C, where the values of the initial and final thicknesses are very close. In addition, the failure strain is much more localized at the higher temperature, corresponding to the typical formation of the fracture neck in the ductile fracture.

The value of P_y, corresponding to the load where the plastic bending regime begins, was obtained from the same load-displacement curves in Fig. 3. Its value was determined by drawing a line parallel to the linear part of the curve at a distance $t/10$ from the origin.[10] Figure 8 shows the evolution of P_y/t^2 and P_{max}/t^2 with temperature.

While P_y/t^2 increases continuously as the temperature decreases, the ductile-to-brittle transition is clearly observed in the P_{max}/t^2 versus temperature plot. As the temperature decreases, P_{max}/t^2 first increases slowly and then more abruptly as it approaches the transition region, attaining a maximum value at −120 °C. It is then possible to use the mean value of P_{max}/t^2 in order to define a new transition temperature. The transition temperature obtained using this last approach is the same as the one obtained from the energy, −125 °C.

As noted above, these two parameters have been respectively associated with the yield stress and the tensile strength of the material through relationships such as Eqs (1) and (2). Table 2 shows the mean values of the steel tensile mechanical properties (yield stress, tensile strength, tensile elongation, and tensile area reduction) obtained at different temperatures, ranging from −60 to +50 °C. In this range of temperatures, the yield stress and tensile strength increase linearly as temperature decreases. Figure 9 compares these two properties with the corresponding SPT parameters, P_y/t^2 and P_{max}/t^2. Very good linear correlations were obtained, giving rise to expressions (5) and (6):

$$\sigma_{ys} = 207 + 0.268 P_y/t^2 (\text{MPa}) \quad -60^\circ\text{C} \le T \le 50^\circ\text{C}, \quad (5)$$

$$\sigma_u = 269 + 0.051 P_{max}/t^2 (\text{MPa}) \quad -60^\circ\text{C} \le T \le 50^\circ\text{C}. \quad (6)$$

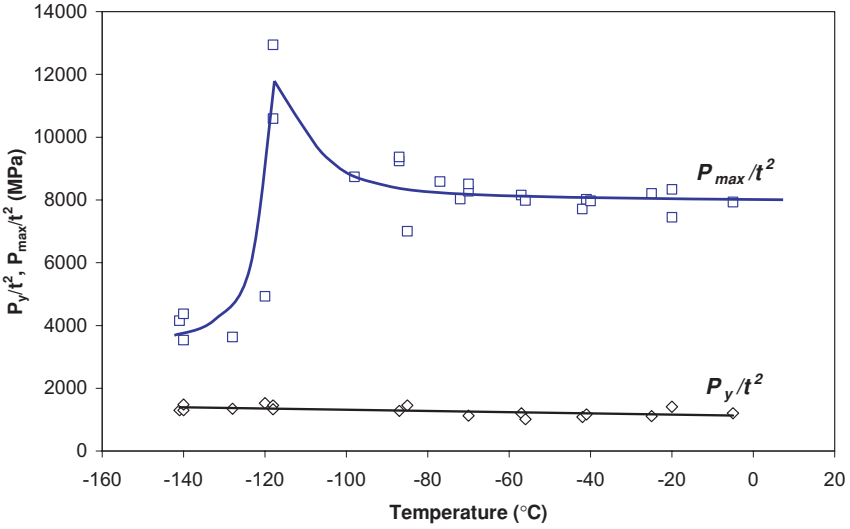

Fig. 8 Variation of P_y/t^2 and P_{max}/t^2 with temperature (AE460).

Table 2 AE460 tensile properties at different test temperatures

Temperature (°C)	−60	−45	−15	0	20	50
σ_{ys} (MPa)	545	535	527	522	515	469
σ_u (MPa)	715	712	692	672	662	657
A (%)	17	19	21	20	22	25
Z (%)	67	67	70	70	71	75

DISCUSSION

As can be seen from Figs 5, 6 and 8, representations as a function of the temperature of the fracture energy, the fracture strain and the maximum load obtained in the SPTs, respectively, clearly show the ductile-to-brittle transition of the material. From each of these curves, it is possible to define a transition temperature corresponding to the mean values of the ductile and brittle plateaus. The values obtained in all three cases are very similar, close to −125 °C. When these curves are compared with the transition curve obtained in the CVN test of the same material, it can be clearly seen that SPT ductile-to-brittle transition takes place at a much lower temperature than the corresponding Charpy transition. This large difference in temperature transition may be justified on the basis of the different nature of the two tests.

In ferritic steels, the final process of fracture at each temperature is the result of competition between two potentially active mechanisms of fracture: cleavage fracture and ductile fracture.

For cleavage to occur, the maximum principal local stress must reach a certain value. This type of fracture will thus be promoted, on the one hand, by the drop in temperature, which increases these local stresses and which is the basis of the ductile-to-brittle transition, and, on the other, by the presence of stress concentrators. The notch in the CVN test specimens therefore favours this embrittlement and the transition will occur at higher temperatures than in the SP tests, where there is no notch. This difference is heightened by the dynamic nature of the CVN test, compared with the static nature of the SP test. The high rates of deformation increase the yield stress of the material, and hence local stresses. Therefore, for the same temperature, the behaviour will be much more brittle in the CVN test, giving rise to the major difference in transition temperature obtained in the two test procedures.

In order to determine the different micromechanisms operating at the different temperatures, a fractographic study of the broken specimens was performed. Figure 10 gives the fracture surface of the SPT specimen tested at −85 °C, which corresponds to the SPT high energy region, as can be seen in Fig. 4. This specimen was extensively plastically deformed before failure, and necking is also clearly visible in the hoop direction (Fig. 10), near the punch-specimen contact, as a consequence of a circumferential constraint imposed by the punch. The fracture pattern in Fig. 10 is characterized by the presence of microcavities typical of ductile failure (initiation, growth and coalescence of microvoids). It should be noted that, according to Fig. 5, the Charpy specimen broken at the same temperature behaved in a completely brittle pattern.

Figure 11 represents the fracture surface of the SPT specimen tested at −140 °C (SPT low energy region, Fig. 4). The failure micromechanism is 100% cleavage as can be expected in the low temperature brittle region. The macroscopic fracture was also quite different, as three

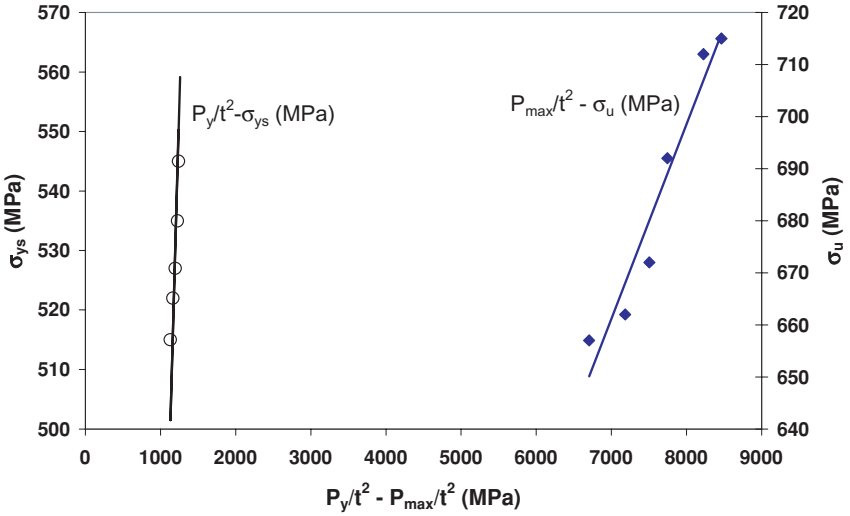

Fig. 9 Correlations between SPT parameters and yield stress and tensile strength.

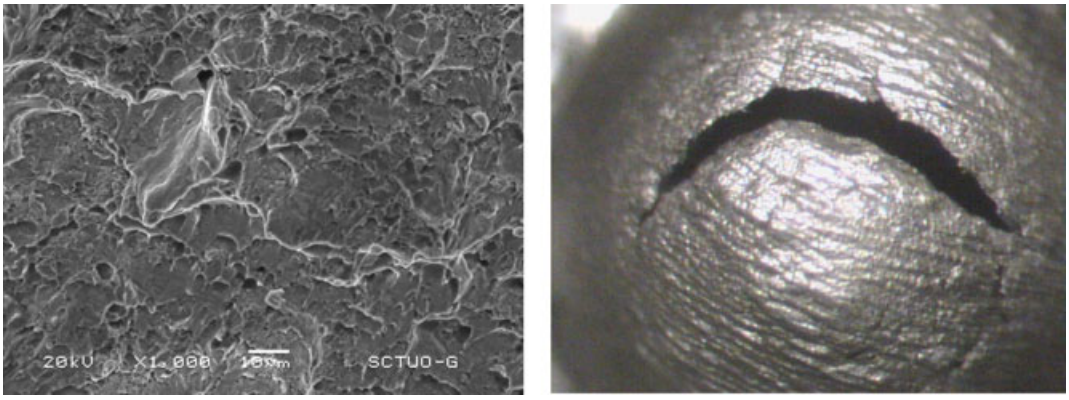

Fig. 10 SPT specimen tested at −85 °C. Ductile surface pattern.

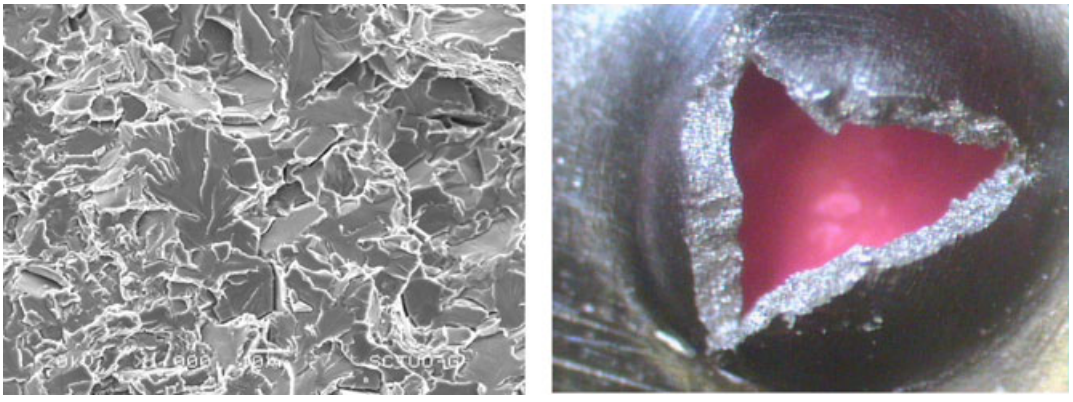

Fig. 11 SPT specimen tested at −140 °C. Brittle surface pattern.

radial cracks suddenly developed given way to significant load drops (Figs 3 and 11), as the circumferential direction is the one corresponding to the maximum stress on bending.

Finally, Fig. 12 corresponds to the SPT specimen tested at −118 °C (transition region according to Fig. 4), where ductile and brittle micromechanisms coexist, as microvoids and cleavage planes are simultaneously observed.

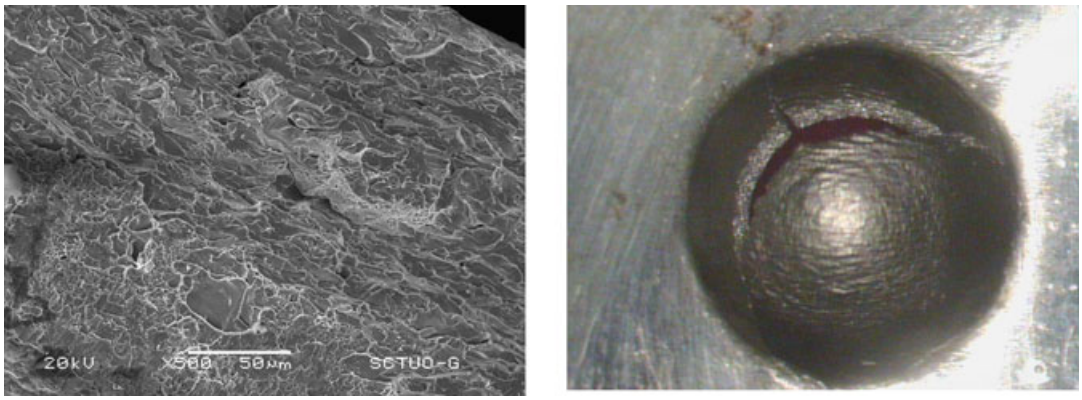

Fig. 12 SPT specimen tested at −118 °C. Surface pattern corresponding to the transition zone.

Table 3 Ductile-to-brittle transition temperatures (DBTT) obtained from Charpy and SPT tests

Small punch test	CVN test			
$DBTT_{SPT}$	$DBTT_{28J}$	$DBTT_{41J}$	$DBTT_{50\%}$	$DBTT_{FATT}$
148 K	213 K	223 K	260 K	261 K
$\gamma = \frac{DBTT_{SPT}}{DBTT_{CVN}}$	γ_{28}	γ_{41}	$\gamma_{50\%}$	γ_{FATT}
	0.69	0.66	0.56	0.56

As noted above, several researchers have linked the transition temperatures obtained via both types of testing by expressions such as (4). Both the SP and the CVN test allow the definition of different temperatures of transition ($DBTT_{SPT}$ for the SP test and $DBTT_{CVN}$, $DBTT_{CVN28J}$, $DBTT_{CVN41J}$, $DBTT_{FATT}$ for the CVN test). Table 3 shows the values of the DBTT obtained in our tests for the different definitions, as well as the γ constant, which correlates SPT and Charpy transition temperatures using an expression such as (4), where the temperatures are expressed in K.

The value of the γ constant depends on the definition of the transition temperature in the CVN test. When it comes to comparing these results with those obtained by other researchers, the most commonly used definition is the $DBTT_{FATT}$. In our case, this value of γ is larger than that obtained by other researchers with ferritic steels ($\gamma \cong 0.4$),[11,12] though similar to the value obtained by Ruan *et al.*[13] ($\gamma = 0.52 \pm 0.12$) with quenched and tempered steels with a similar toughness to our AE460 steel.

As regards the results of mechanical properties, Fig. 13 shows the relations obtained between the yield stress of the material and the parameter P_y/t^2, along with expressions given by other authors for different kinds of steels[12,14–16]. As can be seen, these results are within the range of values provided by other authors. Adjusting these results as a law of the type

$$\sigma_{ys} = \alpha\left(\frac{P_y}{t^2}\right), \tag{7}$$

a value of α equal to 0.43 is obtained, which is between the values of 0.59 and 0.36 given by Cheon *et al.*[14] and Kameda and Mao,[12] respectively. In the first case, the tests were carried out on duplex steels, whereas in the rest of the references the tested steels are more similar to ours. As for the results of Kameda and Mao,[12] the SPT tests were conducted at a much higher displacement velocity (2 mm/min) than in our tests (0.2 mm/min). This difference in velocity led to significant differences in the values of P_y, as has been pointed out by other authors.[11] The values given by Finarelli *et al.*[16] and Campitelli *et al.*[15] for steels that are more similar to ours are 0.38 ± 0.06 and 0.4 ± 0.12, respectively.

In contrast, the relationship between the maximum load obtained in the SPTs and the tensile strength of the material, as indicated in Eq. (6) has to be viewed more cautiously. As we have indicated, the values of the maximum load, and therefore of the constants of Eq. (6), depend on the coefficient of friction between the tested specimen and the punch, as well as other test parameters. This means that this relationship is not generalizable, even for the same material if the test conditions vary, as has already been pointed out by other authors.[15]

CONCLUSIONS

The SPT ductile-to-brittle transition curve of an AE460 structural steel was obtained using three different parameters: the fracture energy (W_f), the local strain at failure location (ε_f) and the test maximum load divided by the square of the initial specimen thickness (P_{max}/t^2). The SPT transition temperature obtained in all cases are much lower than the Charpy transition temperature. This fact can be justified by the major differences in strain rate and

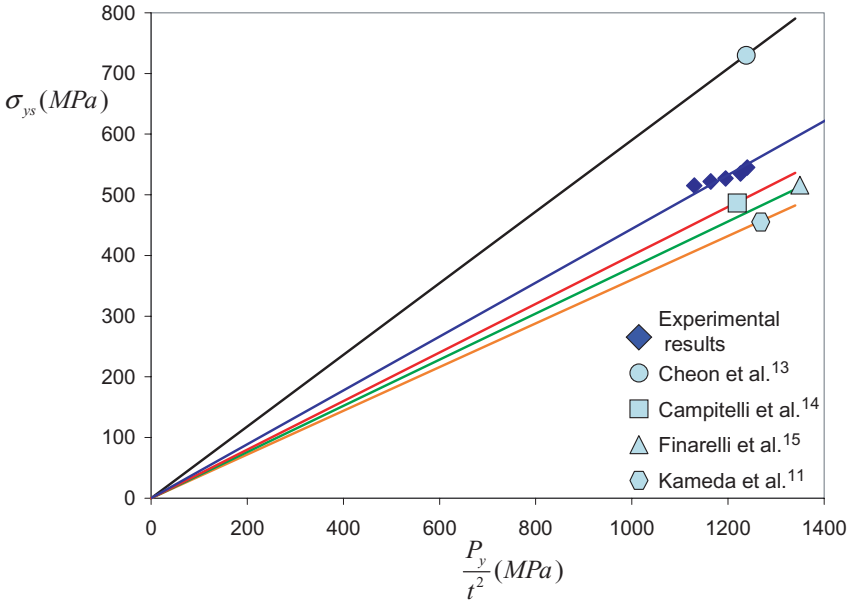

Fig. 13 Experimental and bibliographic relations.[11,13–15] between P_y/t^2 parameter and yield stress for different steels.

stress state characteristics of the two tests. The SPT is a static test and the stress state at failure is biaxial (plane stress), while the CVN test is dynamic and subjected to triaxial stresses.

The ductile-to-brittle transition obtained with the AE460 steel using energy or maximum load criteria starts at about −120 °C and extends until the minimum test temperature used in the study, −140 °C. However, this transition appears at higher temperatures (from −90 to −130 °C) when it is obtained from the local strain at the failure site. Fractographic analysis was used to identify the failure micromechanisms operating at the different SPT temperatures: ductile micromechanisms consisting of the initiation, growth and coalescence of microvoids were always observed in the high energy region ($T \geq -100$ °C), brittle cleavage micromechanisms were operative in the low energy region ($T \leq -140$ °C), with a mixture of both in the transition zone between the aforementioned temperatures.

The transition temperature correlation between Charpy and SPT tests gives rise to the following expression:

$$\mathrm{DBTT_{SPT}} = 0.56\ \mathrm{DBTT_{FATT}} (\text{both temperatures in } K). \quad (8)$$

The P_{max}/t^2 also shows a ductile-to-brittle temperature transition, but the SPT parameter directly related to the yield strength, Py/t^2, increases linearly as the test temperature decreases (at least until −140 °C).

Between −60 and +50 °C, the SPT parameters, P_y/t^2 and P_{max}/t^2, and their corresponding tensile properties, σ_{ys} and σ_u, present linear correlations with very low dispersion. The relation obtained for P_y/t^2 is within the range of values found in the literature. On the other hand, the relation obtained for P_{max}/t^2, must be considered dependent on test conditions.

Acknowledgements

The authors gratefully acknowledge funding from the Spanish Science and Education Ministry provided via project DGICYT (MAT-2004-06992-C02-01).

REFERENCES

1 Lucon, E. (2001) Material damage evaluation and residual life assessment of primary power plant components using specimens of non-standard dimensions. *Mater. Sci. Tech.* **17**, 77–785.
2 Fleury, E. and Ha, J. S. (1998) Small punch tests to estimate the mechanical properties of steels for steam power plant. *Int. J. Press. Ves. Pip.* **75**, 699–706.
3 Hosford, W. F. and Caddel, R. M. (1983) *Metal Forming: Mechanics and Metallurgy*. Prentice-Hall Inc., London.
4 Vorliceck, V., Exworthy, L. F. and Flewitt, P. E. J. (1995) Evaluation of a miniaturized disc test for establishing the mechanical properties of low alloy steels. *J. Mater. Sci.* **30**, 2936–2943.
5 Song, S. H. Faulkner, R. G., Flewitt, P. E. J., Smith, R. F. and Marmy, P. (2000) Temper embritlement of a CrMo low-alloy steel evaluated by means of small punch testing. *Mat. Sci. Eng.* **A281**, 75–81.
6 Foulds, J. and Viswanatham, R. (2001) Determination of in-service steam turbine disks using small punch testing. *J. Mat. Eng. Perform.* **10**, 614–619.
7 Bulloch, J. H. (2002) A review of the ESB small punch test data on various plant components with special emphasis on fractographic details. *Eng. Fract. Anal.* **9**, 511–534.

8 Gai, X. Sato, S., Kokawa, H. and Ichikawa, K. (2002) Ductile-brittle transition of steel electron beam weld metal in small punch. *Sci. Tech. Weld. Join.* **7**, 204–211.
9 Autillo, J., Contreras, M. A., Betegón, C., Rodríguez, C. and Belzunce, F. J., (2006) Utilización del ensayo miniatura de punzonamiento en la caracterización mecánica de aceros. *Anales de Mecánica de la Fractura* **23**, 77–83.
10 Cheon, S. and Kim, I. S. (1996) Initial deformation during small punch test. *J. Test. Eval.* **24**, 255–262
11 Saucedo-Muñoz, M. L., Komazaki, S. I., Hashida, T., Shoji, T. and López-Hirata, V. M. (2003) Aplicación del ensayo miniatura de embutido para la evaluación de la tenacidad a temperaturas criogénicas de aceros inoxidables austeníticos envejecidos térmicamente. *Rev. Met. Madrid* **39**, 378–386.
12 Kameda, J. and Mao, X. (1992) Small-punch and TEM – disc testing techniques and their application to characterization of radiation damage. *J. Mat. Sci.* **27**, 983–989.
13 Ruan, Y., Spatig, P. and Victoria, M. (2002) Assessment of mechanical properties of the martensitic steel EUROFER97 by means of punch tests. *J. Nucl. Mater.* **307**, 236–239.
14 Cheon, Y. S. and Kim, I. S. (2000) Evaluation of thermal aging embrittlement in CF8 duplex stainless steel by small punch test. *J. Nucl. Mater.* **278**, 96–103.
15 Campitelli, E., Spatig, P., Bonade, R., Hoffelner, W. and Victoria, M. (2004) Assessment of the constitutive properties from small ball punch test: experimental and modelling. *J. Nucl. Mater.* **335**, 366–378.
16 Finarelli, D., Roeding, M. and Carsughi, F. (2004) Small punch tests on austenitic and martensitic steels irradiated in a spallation environment with 530 MeV portons. *J. Nucl. Mater.* **328**, 146–150.

